Chen *et al.*
European Journal of Medical Research (2025) 30:141
https://doi.org/10.1186/s40001-025-02359-z

European Journal of Medical Research

RESEARCH Open Access

circZNF707 promoted glycolysis and tumor progression through miR-668-3p-PFKM axis in NSCLC

Wei Chen[1,2†], Shuai Fang[1†], Xianqiao Wu[1,2], Tianzheng Fang[1,2], Ziyuan Chen[1,2], Wenmin Su[1], Yuchao Zhu[3], Xiaodong Zhao[1,2*] and Chengwei Zhou[1,2*]

Abstract

Background Circular RNA (circRNA) plays an important regulatory role in the development of human malignancies, but the potential mechanisms of circRNA in non-small cell lung cancer (NSCLC) remain largely unknown.

Methods Microarray analysis was used to test for circRNAs differing in expression between NSCLC tumors and healthy adjacent tissues. Using qRT-PCR, the expression of circZNF707 was determined. Through a number of loss-of-function and gain-of-function investigations, the biological behavior of NSCLC cells was evaluated. Finally, tests using Western blotting, RIP, qRT-PCR, and luciferase reporter gene detection and rescue assays revealed the potential mechanism of circZNF707.

Results Increased expression of circZNF707 was found in NSCLC tissues. Functionally, circZNF707 enhances proliferation, migration, invasion, and glycolysis of NSCLC cells. Mechanistically, circZNF707 can upregulate PFKM by acting as a sponge for miR-668-3p, thus contributing to the progression of NSCLC.

Conclusions Through the circZNF707/miR-668-3p/PFKM axis, upregulation of circZNF707 promotes tumor development. CircZNF707 may provide new insights into the treatment and diagnosis of NSCLC.

Keywords CircRNA, MiR-668-3p, PFKM, NSCLC, Glycolysis

Introduction

Non-small cell lung cancer (NSCLC) is a highly burdensome malignant tumor worldwide and has a significant impact on human health [1]. I In recent years, new treatment methods including targeted therapy, anti-tumor angiogenic drugs, and immune checkpoint inhibitors have emerged, yet NSCLC continues to pose a challenge in tumor treatment [2, 3]. Glycolysis fulfills the energy requirements of tumor cells while simultaneously affecting the tumor microenvironment via its metabolic byproducts, positioning it as a promising therapeutic target, with PFKM recognized as a key regulatory enzyme in the glycolytic pathway. Hence, investigating the molecular mechanisms underlying the development of NSCLC and discovering novel early diagnostic markers and therapeutic targets are of utmost importance.

†Wei Chen and Shuai Fang have contributed equally to this work.

*Correspondence:
Xiaodong Zhao
zhxido@sohu.com
Chengwei Zhou
fyzhouchengwei@nbu.edu.cn
[1] Thoracic Surgery Department, The First Affiliated Hospital of Ningbo University, No.247 Renmin Road, Ningbo 315020, Zhejiang Province, People's Republic of China
[2] Ningbo University School of Medicine, Ningbo, Zhejiang Province, People's Republic of China
[3] State Key Laboratory of Agricultural Microbiology, College of Veterinary Medicine, Huazhong Agricultural University, Wuhan, Hubei Province, People's Republic of China

Circular RNA (circRNA) is a unique subtype of non-coding RNA (ncRNA) that has become a prominent area of focus in RNA research [4–6]. CircRNA forms a specific covalently closed loop structure, lacking polarity from 5' to 3', and polyadenylation tails [7]. Moreover, circRNA exhibits tissue and cell-specific expression, suggesting a crucial regulatory role in diverse biological and pathological processes [8]. Recent studies have revealed the involvement of circRNA in the development of various cancers, such as gastric cancer, pancreatic cancer, lung cancer, breast cancer, and bladder cancer, by modulating different cellular processes [9–12]. As previously reported, circTP63 can upregulate the expression of forkhead box M1 (FOXM1) by sequestering miR-873-3p, thereby promoting cancer cell proliferation [13]. CircSATB2 as a positive regulator of muscle-specific actin-binding protein 1 (FSCN1) expression through miR-326 in NSCLC cells [14]. Furthermore, circSATB2 can be transported via exosomes, promoting the proliferation, migration, and invasion of NSCLC cells, as well as inducing abnormal proliferation in normal human bronchial epithelial cells. Nonetheless, the specific roles of most circRNAs in the progression of lung cancer remain unclear and necessitate further exploration.

To elucidate the function of circRNA in NSCLC, we selected circRNAs from the GEO datasets (GSE101684 and GSE101586). By selecting circRNAs with large differential expression from the two databases, it can be found that circZNF707 is the only circRNA in the two GSE datasets. Therefore, circZNF707 was selected for further study. We identified a novel circRNA, circZNF707, derived from exons 2 and 3 of the ZNF707 gene, which was upregulated in NSCLC tissues and cell lines. Furthermore, functional experiments demonstrated that circZNF707 promotes the proliferation, migration, invasion, and glycolysis of NSCLC cells. Mechanistically, we found that circZNF707 sequesters miR-668-3p, attenuating its inhibitory effect on PFKM mRNA expression, thereby activating glycolysis in NSCLC cells, and promoting NSCLC progression.

Materials and methods

Patient tissue samples

At the First Affiliated Hospital of Ningbo University (Ningbo, China), 50 NSCLC patients' tumour tissue and adjacent tissue samples were taken. Multiple attending physicians made the lung cancer diagnosis for each patient. Patients with other cancers or those who have received radiation or chemotherapy in the past were not eligible. The specimens were obtained from tumor surgical resections, approximately the size of a 45 mg soybean (with a diameter of about 6–8 mm). The adjacent normal tissues were collected from areas at least 5 cm away from the tumor margins, significantly reducing the likelihood of contamination with tumor cells within the normal tissue. The samples were immediately placed in liquid nitrogen after collecting and kept there until further examination. Additionally, general clinical data and thorough pathology records were gathered. All patients gave their informed consent. The First Affiliated Hospital of Ningbo University's Clinical Research Ethics Committee gave the study protocol approval (Approval No.: KS202112011). All experimental methods were carried out in compliance with the applicable laws. The clinical characteristics of all patients (age, gender, smoking history, tumor size, histological subtype, differentiation grade, TNM stage, lymph node metastasis, and distant metastasis) are shown in Table S3.

The detailed methods for the cell culture, cell transfection, RNase R assays, Nucleocytoplasmic fractionation, cell counting Kit-8 assay, wound healing assay, transwell assay, dual-Luciferase reporter Gene assay, RNA immunoprecipitation assay, western blotting and statistical analysis are described in Appendix S1.

Results

Expression and subcellular localization of circZNF707 in NSCLC tissues and cells

We obtained lung cancer chip data from the GEO database (GSE101586 and GSE101684) and conducted bioinformatics analysis to generate volcano plots (Fig. 1A, B), illustrating the differential expression of circRNA in NSCLC tissues compared to adjacent tissues. Upon applying the criteria of $P < 0.05$ and Fold Change > 1.5 to the two datasets, we identified elevated levels of circZNF707 (hsa_circ_0006566) in both chip datasets (Fig. 1C). The elevated expression of circZNF707 in NSCLC tissues compared to adjacent tissues was validated in 50 pairs of NSCLC tissues (Fig. 1D, E), consistent with the chip results. Subsequent confirmation of circZNF707 expression in human normal lung epithelial cells BEAS-2B, bronchial epithelial cells HBE, and NSCLC cells (SPC-A-1, NCI-H69, NCI-H446, NCI-H1299, and A549) revealed a significant increase in NSCLC cells compared to bronchial epithelial and normal lung epithelial cells (Fig. 1F). Therefore, A549 with relatively high expression and NCI-H1299 with low expression were chosen as experimental cell lines for further investigations. The circRNA molecule circZNF707 originates from the 2nd and 3rd exons of the zinc finger protein 707 (ZNF707) gene on human chromosome 8 (Fig. 1G).

Previous research has suggested that due to its stable closed-loop structure, circRNA is resistant to degradation by exonucleases. To confirm the stability of circZNF707, we conducted experiments using RNase R (Fig. 1H) and actinomycin D (Fig. 1I), demonstrating

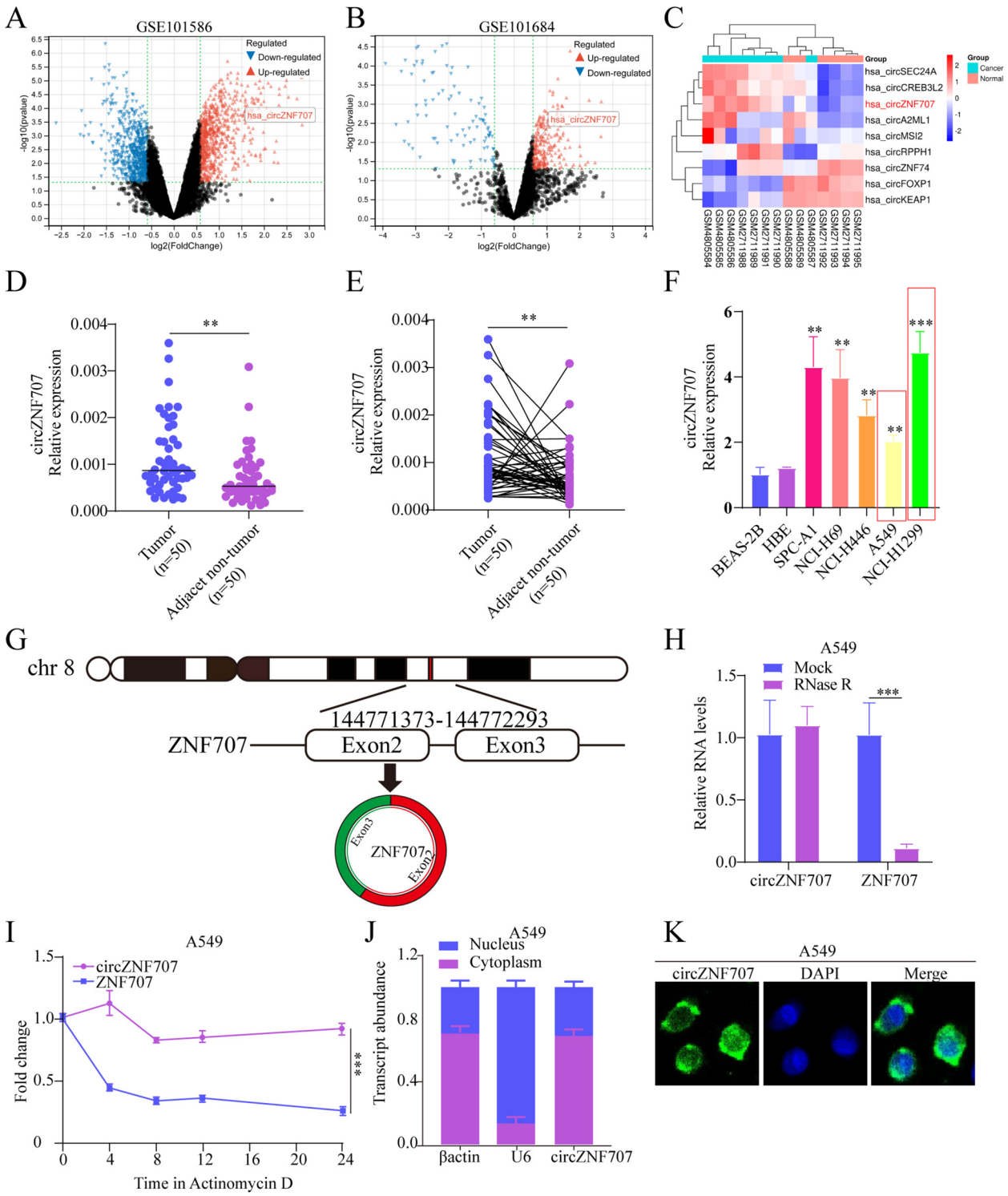

Fig. 1 Expression and characteristics of circZNF707 in NSCLC. **A** Differentially expressed circRNA in GSE101586 dataset. **B** Differentially expressed circRNA in GSE101684 dataset. **C** Heatmap of differentially expressed circRNA in GSE101586 and GSE101684 datasets. **D**, **E** Expression levels of circZNF707 detected by qRT-PCR in NSCLC and adjacent tissues. **F** Expression levels of circZNF707 detected by qRT-PCR in normal human lung epithelial cells, bronchial epithelial cells, and NSCLC cell lines. **G** circZNF707 formed by reverse splicing of exons 2 and 3 of the ZNF707 gene. **H** Expression of circZNF707 and ZNF707 mRNA detected by qRT-PCR after RNase R treatment in A549 cells. **I** Expression levels of circZNF707 and ZNF707 mRNA detected by qRT-PCR after resveratrol D treatment in A549 cells. **J** Expression levels of circZNF707 detected by qRT-PCR in the cytoplasm and nucleus of A549 cells. **K** FISH staining confirmed the expression of circZNF707 in the cytoplasm. Scale bar, 100 μm. $^{**}P < 0.01$, $^{***}P < 0.001$

that the expression level of circZNF707 remained relatively unchanged, while the linear ZNF707 mRNA showed a significant decrease. Additionally, FISH and cytoplasmic fractionation assays indicated that circZNF707 is predominantly located in the cytoplasm of NSCLC cells, with approximately 75% found in the cytoplasm and 25% in the nucleus of A549 cells (Fig. 1J). FISH tests further confirmed the cytoplasmic abundance of circZNF707 (Fig. 1K).

circZNF707 promotes proliferation, migration, invasion, and glycolysis of cells in vitro

The efficiency of circZNF707 overexpression in the NCI-H1299 cell line and the effectiveness of si-circZNF707 silencing in the A549 cell line were assessed using qRT-PCR analysis (Fig. 2A, B). Subsequent investigations revealed that ectopic expression of circZNF707 led to increased cell viability in NCI-H1299 cells, while knockdown of circZNF707 had the opposite effect (Fig. 2C–E). Furthermore, overexpression of circZNF707 promoted cell migration, invasion, and glycolysis, whereas silencing of circZNF707 resulted in the opposite effects (Fig. 3A–G).

circZNF707 acts as a sponge for miR-668-3p in NSCLC

Numerous studies have demonstrated that competitive interaction between miRNA and circRNA controls the subcellular location of circRNA in the cytoplasm, which in turn controls tumor growth by modifying mRNA expression [15, 16]. We predicted the potential miRNAs

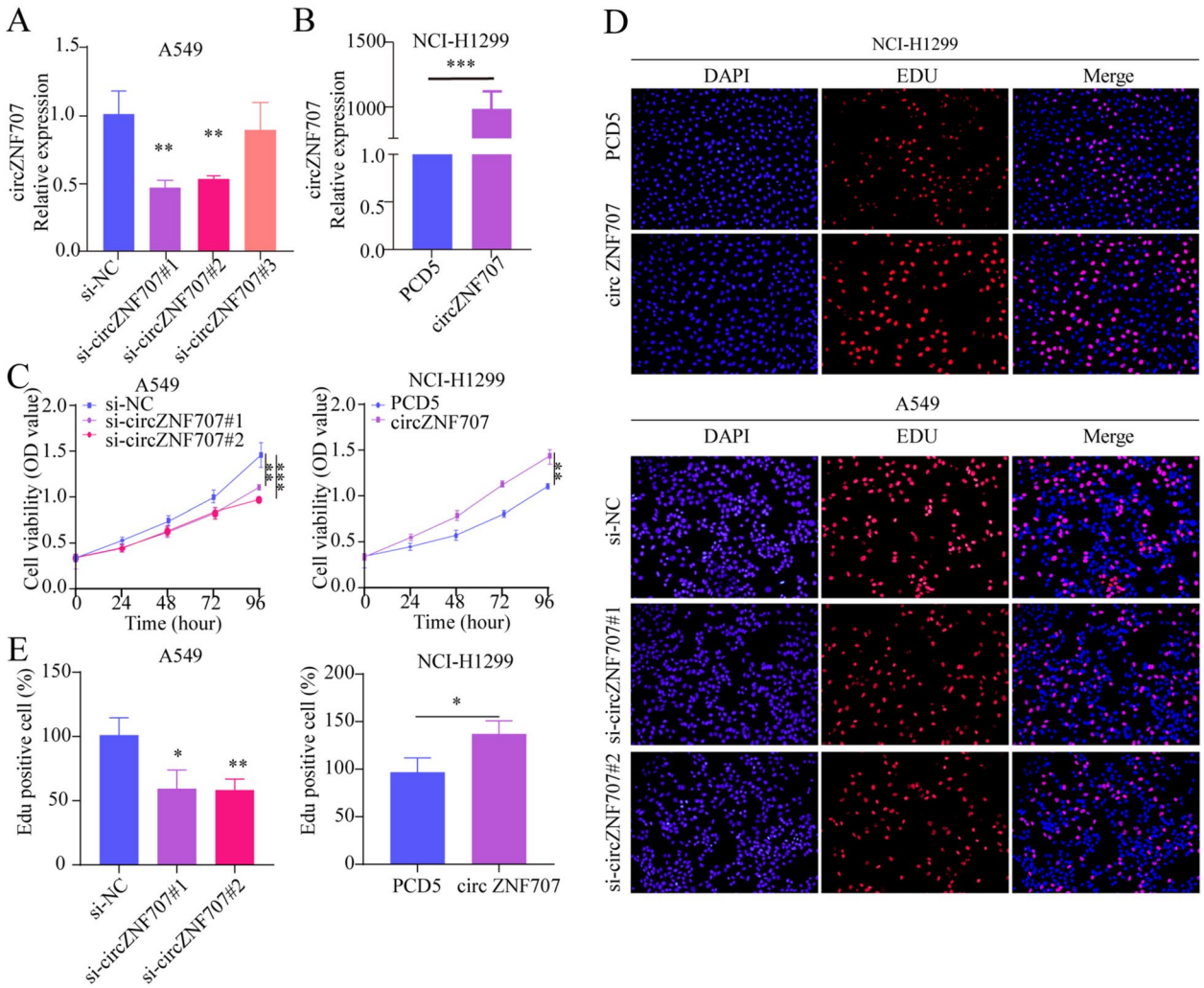

Fig. 2 circZNF707 promotes cell proliferation in vitro. **A** Transfection of siRNA in A549 cells and qRT-PCR detection of circZNF707 expression levels. **B** Transfection of circZNF707 overexpression vector in NCI-H1299 cells and qRT-PCR detection of circZNF707 expression levels. **C**–**E** CCK-8 and EDU assays to assess the proliferation ability of NSCLC cells after circZNF707 overexpression or knockdown. *$P < 0.05$, **$P < 0.01$, ***$P < 0.001$

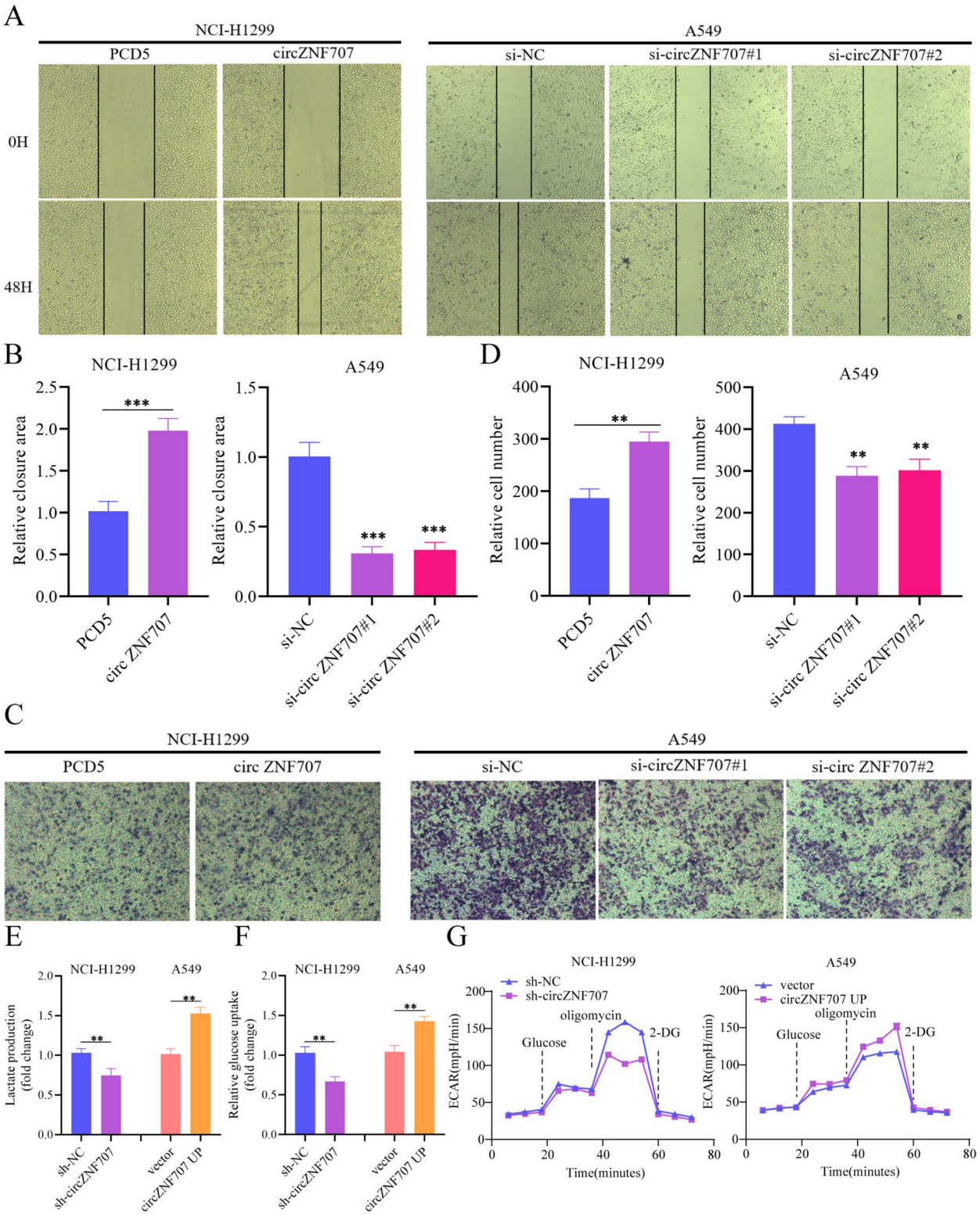

Fig. 3 circZNF707 enhances cell migration and invasion ability in vitro. **A**–**D** Wound healing and Transwell assays to evaluate the migration and invasion ability of NSCLC cells after circZNF707 overexpression or knockdown. Scale bar, 100 μm. **E**, **F** Measurement of lactate and glucose uptake in NSCLC cells after circZNF707 overexpression or knockdown. **G** Analysis of extracellular acidification rate (ECAR) using a Seahorse analyzer after circZNF707 overexpression or knockdown. *$P < 0.05$, **$P < 0.01$, ***$P < 0.001$

that could bind to circZNF707 using the databases miRanda, Circinteractome, and RNAhybrid (Fig. 4A). When the information from these three databases was combined, the findings suggested that miR-326, miR-330, and miR-668-3p might be able to bind to circZNF707 downstream. After circZNF707 was knocked down in A549 cells, qRT-PCR tests were performed to confirm the expression levels of miR-326, miR-330, and miR-668-3p. The findings demonstrated that miR-668-3p's expression level was the only one that had increased. In contrast, only the expression level of miR-668-3p was downregulated in NCI-H1299 cells following overexpression (Fig. 4B, C). To confirm the binding capability of circZNF707 and miR-668-3p, we used an AGO2 antibody for RNA immunoprecipitation. The results showed that the AGO2 group had significantly more miR-668-3p and circZNF707 binding than the control group IgG (Fig. 4D–F). In addition, we created a luciferase reporter gene plasmid by fusing the vector with the linear sequence of miR-668-3p of circZNF707 or a sequence with a predicted binding site mutation (Fig. 4G). The direct binding of circZNF707 and miR-668-3p was confirmed using dual luciferase reporter gene assays (Fig. 4H). Importantly, we used qRT-PCR to identify the expression of miR-668-3p in NSCLC tissues, and the results revealed that the expression of miR-668-3p in NSCLC tissues was much lower than in normal adjacent tissues (Fig. 4I). Pearson correlation analysis revealed a negative relationship between miR-668-3p and circZNF707 expression in NSCLC tissues (Fig. 4J). These findings suggest that in NSCLC, circZNF707 works as a molecular sponge for miR-668-3p.

We designed rescue studies to see if circZNF707 is regulated by miR-668-3p in the progression of NSCLC. Co-transfection of pCD5-circZNF707 and miR-668-3p mimics into NCI-H1299 cells (Fig. 5A–D) and si-circZNF707 and miR-668-3p inhibitors into A549 cells was used to assess the biological functions of each group of cells (Figure S1A-D). The results shown that miR-668-3p can reverse the stimulating effect of circZNF707 on NSCLC cell proliferation, migration, and invasion. In conclusion, circZNF707 can promote tumor progression in NSCLC by acting as a molecular sponge for miR-668-3p.

PFKM is a downstream target of miR-668-3p

MiRNAs inhibit the transcription and translation of target genes by binding to the 3'UTR of their downstream target genes, thereby exerting their biological functions [17–19]. We transfected miR-668-3p mimic and miRNA-NC control into NCI-H1299 cells and detected the expression changes of downstream genes using RNA sequencing. The results showed significant changes in the expression of genes such as JAM3, NR1H4, DDX43, TSPAN12, AOC1, and PFKM (Fig. 6A). Meanwhile, we used PITA, miRmap, microT, and TargetScan databases to analyze the downstream target genes of miR-668-3p. The results showed that 26 genes with potential binding sites for miR-668-3p were predicted by the four databases. Simultaneously, we evaluated the 26 potential genes to the RNA sequencing findings and discovered that only the expression level of PFKM changed significantly (Fig. 6B). Based on these findings, we overexpressed miR-668-3p and circZNF707 in NCI-H1299 cells, and the results showed that, as compared to the miRNA-NC control group, miR-668-3p overexpression dramatically reduced PFKM expression (Fig. 6C). Overexpression of circZNF707, on the other hand, greatly boosted PFKM expression. MiR-668-3p and circZNF707 knockdown had the opposite effect (Fig. 6D).

In addition, we created a luciferase reporter gene plasmid by fusing the vector with the linear sequence of PFKM's binding site for miR-668-3p or the sequence with a predicted binding site mutation (Fig. 6E). The direct binding of PFKM and miR-668-3p was verified using a dual luciferase reporter gene assay (Fig. 6F). Meanwhile, qRT-PCR or Western Blot were employed to detect the amount of PFKM gene expression in NSCLC tissues and cells. The results demonstrated that the expression level of the PFKM gene was dramatically upregulated in NSCLC tissues and cells when compared to the control group (Fig. 6G–I). Pearson correlation analysis revealed a positive relationship between PFKM and circZNF707 expression in NSCLC tissues (Fig. 6J). This suggests that

(See figure on next page.)

Fig. 4 circZNF707 functions as a sponge for miR-668-3p. **A** Prediction of potential miRNAs binding to circZNF707 by miRanda, Circinteractome, and RNAhybrid databases. **B** qRT-PCR detection of the expression levels of miR-326, miR-330, and miR-668-3p in NCI-H1299 cells transfected with circZNF707 overexpression vector. **C** qRT-PCR detection of the expression levels of miR-326, miR-330, and miR-668-3p in A549 cells transfected with siRNA. **D** Protein expression levels of AGO2 and ACTIN detected by Western Blot experiment. **E**, **F** Co-immunoprecipitation of AGO2 group and IgG group, with qRT-PCR detection of the expression levels of miR-668-3p and circZNF707. **G** Prediction of the binding site between miR-668-3p and circZNF707 by Circinteractome database. **H** Luciferase assay to detect the binding between miR-668-3p and circZNF707. **I** qRT-PCR detection of the expression levels of miR-668-3p in NSCLC and adjacent tissues. **J** Pearson correlation analysis of the expression correlation between miR-668-3p and circZNF707 in NSCLC tissues. $^{*}P < 0.05$, $^{**}P < 0.01$, $^{***}P < 0.001$

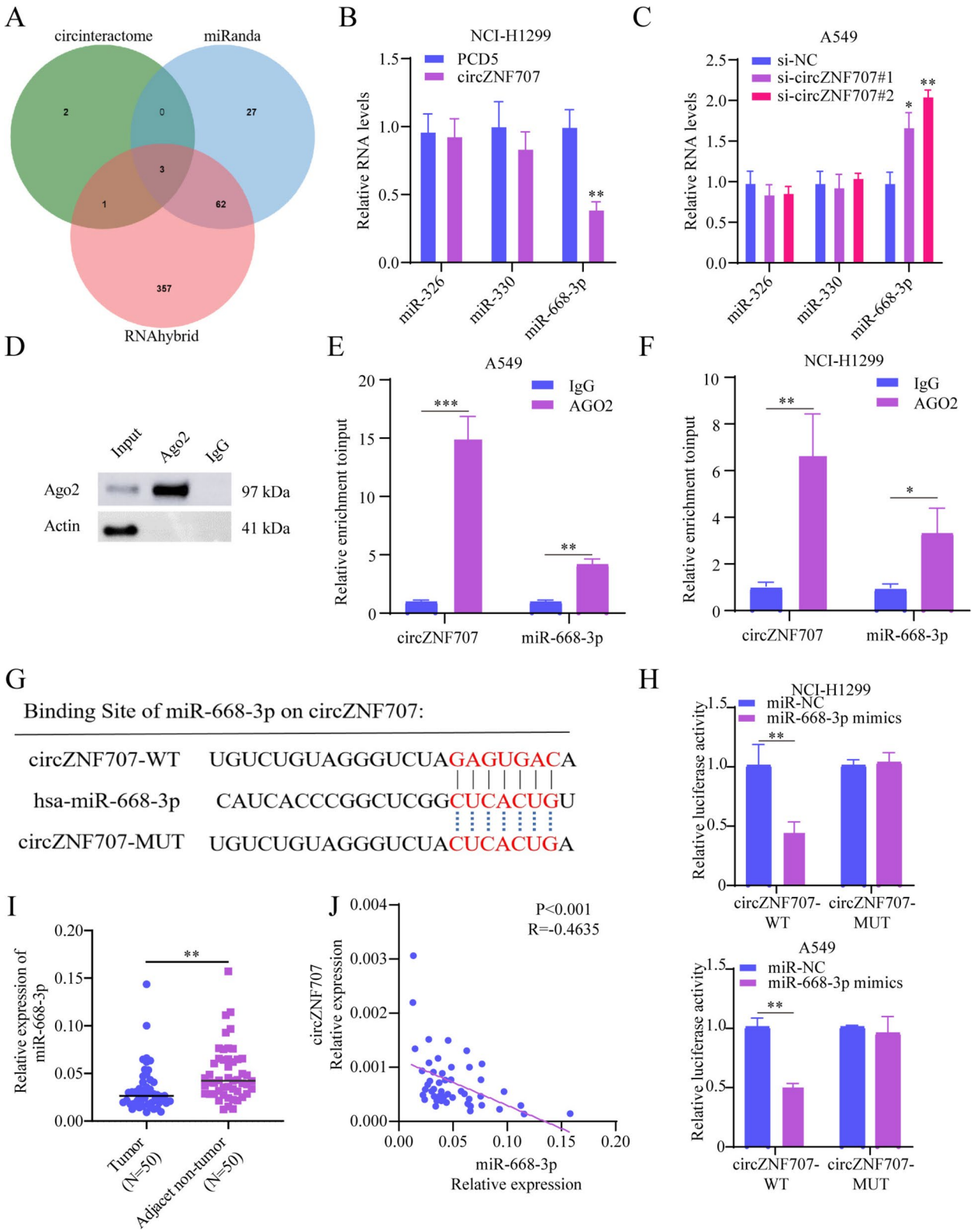

Fig. 4 (See legend on previous page.)

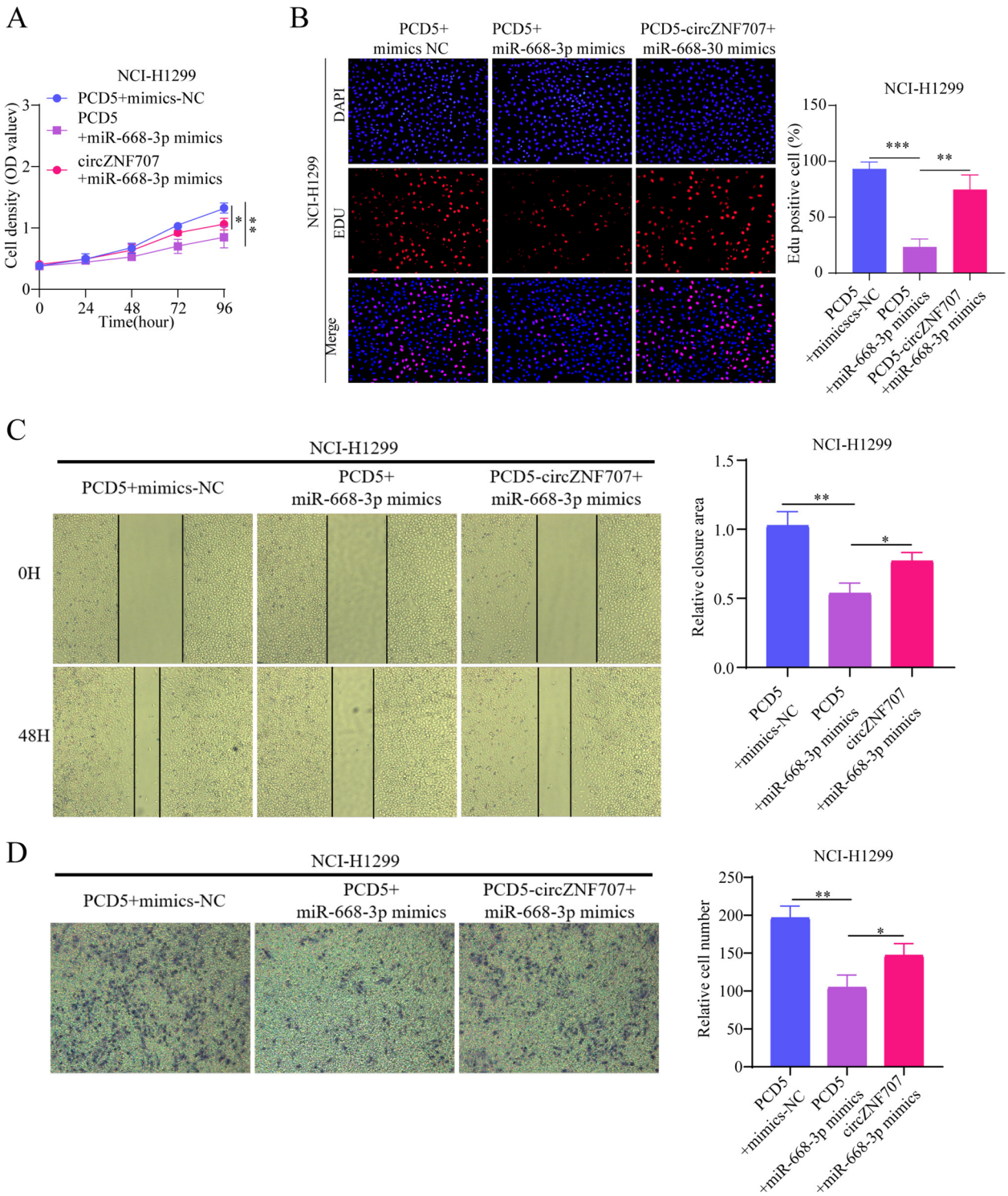

Fig. 5 circZNF707's oncogenic effect in NSCLC can be reversed by miR-668-3p. After transfection with PCD5 + mimics-NC, PCD5 + miR-668-3pmimics, and PCD5-circZNF707 + miR-668-3pmimics in NCI-H1299 cells, **A**, **B** CCK-8 and EDU experiments were conducted to assess cell proliferation ability. **C**, **D** Wound healing and Transwell experiments were performed to evaluate the migration and invasion capability of NSCLC cells. Scale bar, 100 μm. *$P < 0.05$, **$P < 0.01$, ***$P < 0.001$

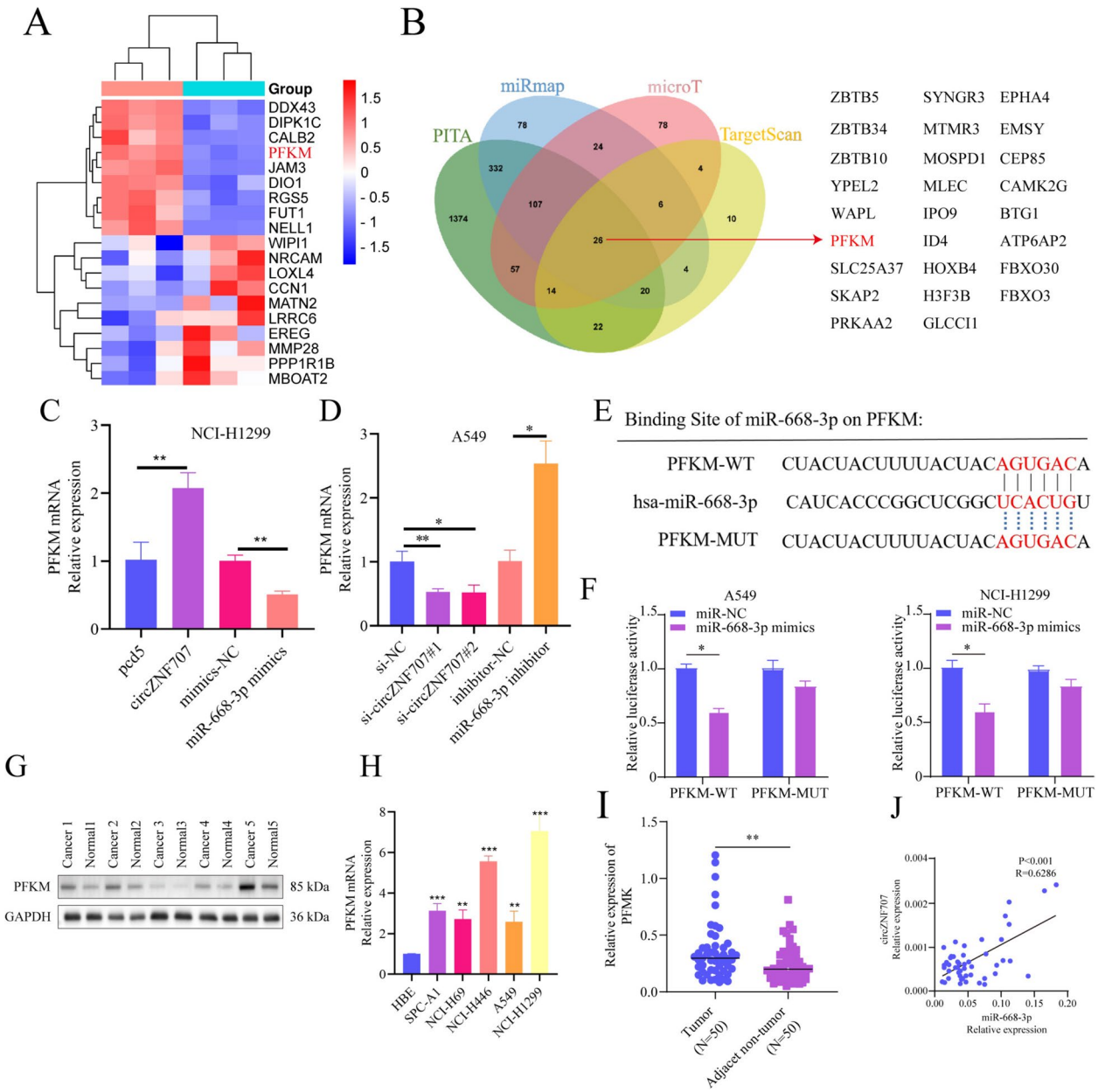

Fig. 6 PFKM is a downstream target gene of miR-668-3p. **A** The expression levels of downstream genes were measured by transcriptome sequencing after transfection of miR-668-3p mimic and miRNA-NC in NCI-H1299 cells. **B** Target genes potentially binding to miR-668-3p predicted by PITA, miRmap, microT, and TargetScan databases. **C** The expression level of PFKM was detected by qRT-PCR after transfection of miR-668-3p mimic and circZNF707 overexpression vector in NCI-H1299 cells. **D** The expression level of PFKM was detected by qRT-PCR and Western Blot after transfection of miR-668-3p inhibitor and circZNF707 siRNA in A549 cells. **E** Predicted binding sites of miR-668-3p with PFKM according to TargetScan database. **F** Luciferase assay to detect the binding sites between miR-668-3p and PFKM. **G** Expression levels of PFKM in NSCLC and adjacent tissue detected by Western Blot. **H** Expression levels of PFKM in human bronchial epithelial cells and NSCLC cell lines detected by qRT-PCR. **I** Expression levels of PFKM in NSCLC and adjacent tissue detected by qRT-PCR. **J** Pearson correlation analysis of the expression correlation between PFKM and circZNF707 in NSCLC tissues. **P* < 0.05, ***P* < 0.01, ****P* < 0.001

the circZNF707/miR-668-3p/PFKM pathway plays a key role in the occurrence and progression of NSCLC.

Finally, it was validated that circZNF707 regulates the expression of PFKM by modulating miR-668-3p, thereby promoting the progression of non-small cell lung cancer (NSCLC). The findings of co-transfection of A549 cells with miR-668-3p inhibitor and by si-PFKM revealed that si-PFKM dramatically inhibited miR-668-3p inhibitor's promoter effects on NSCLC cell proliferation, migration, invasion, and glycolysis (Fig. 7A–G). Similarly, co-transfecting miR-668-3p mimics and PFKM overexpression vector into NCI-H1299 cells demonstrated that the miR-668-3p overexpression could counteract the stimulating effects of PFKM overexpression on NSCLC cell proliferation, migration, invasion, and glycolysis (Figure S2A-G).

circZNF707/miR-668-3p/PFKM axis promotes glycolysis in NSCLC cells

We knocked down circZNF707 in A549 cells and detected the protein levels of glycolytic enzymes, including PFKM, hexokinase 1 (HK1), glyceraldehyde-3-phosphate dehydrogenase (GAPDH), and lactate dehydrogenase A (LDHA), which are key enzymes required for the Warburg effect of converting pyruvate to lactate. Among all detectable proteins, the amount of PFKM protein reduced considerably, but HK1 and LDHA expression remained unchanged (Fig. 8A). More notably, we found that overexpressing miR-668-3p in NCI-H1299 cells resulted in a substantial decrease in PFKM protein levels. However, simultaneous overexpression of circZNF707 restored PFKM protein expression (Fig. 8B–D). In contrast, knocking down both miR-668-3p and circZNF707 had the opposite effect (Fig. 8E).

Knockdown of circZNF707 inhibits the progression of NSCLC in vivo

In the subcutaneous tissue of BALB/c nude mice, we stably implanted A549 cell lines expressing sh-circZNF707 or sh-NC. Tumor size was measured every 3 days, and the mice were killed after 33 days. The experimental results demonstrated that knocking down circZNF707 resulted in a considerable reduction in tumour volume and bulk (Fig. 9A–C). Following circZNF707 knockdown in the cells, Western blot examination of subcutaneous tumour tissue indicated a substantial downregulation of PFKM expression (Fig. 9D). After circZNF707 knockdown, qRT-PCR findings revealed a significant decrease in PFKM expression and an increase in miR-668-3p expression (Fig. 9E). Immunohistochemical staining revealed a substantial decrease in PFKM, CD31, and Ki67 expression levels in tumour tissues from the sh-circZNF707 group compared to the sh-NC group (Fig. 9F).

In conclusion, circZNF707 operates as an oncogene in NSCLC cells by competitively binding to miR-668-3p, increasing PFKM expression, and facilitating glycolysis.

Discussion

The dysregulation of circRNAs in various malignancies has been validated by an increasing number of studies in recent years, which have also clarified their role in the complex control of cellular processes [20, 21]. However, little is known about the particular roles played by circRNAs in NSCLC, necessitating more research. Here, we discovered circZNF707, a new circRNA created by backsplicing exons 2 and 3 of the parental gene ZNF70 to create a closed circular RNA molecule. Our findings show that circZNF707 is significantly upregulated in NSCLC tissues and cells, indicating an oncogenic function. According to the study, circZNF707 overexpression greatly encourages proliferation, migration, invasion, and glycolysis. On the other hand, NSCLC cells' proliferation, migration, invasion, and glycolysis are markedly reduced when circZNF707 is knocked down. Therefore, we speculate that circZNF707 is essential for controlling NSCLC cell proliferation, invasion, and glycolysis.

Existing research indicates that the subcellular localisation of circRNAs plays a significant role in the biological actions of these molecules [22]. CircRNAs' primary biological role is related to their interaction with miRNAs when they are mostly found in the cytoplasm [23, 24]. For instance, by circBCAR3 targets the miR-27a-3p/TNPO1 axis and is predominantly found in the cytoplasm of esophageal cancer cells, where it encourages invasion, metastasis, and treatment resistance [17]. Contrarily, when circRNAs are found in the nucleus, their primary role is to attach to RNA-binding proteins and control the transcription of genes. For instance, by circMRPS35 can localize in the nucleus of gastric cancer cells and specifically bind to the FOXO1/3a promoter, promoting their transcription and translation as well as activating the expression of E-cadherin, p21, and p27, preventing the growth and metastasis of gastric cancer cells [25].

Therefore, to further investigate the role of circZNF707 in the progression of NSCLC, we did a

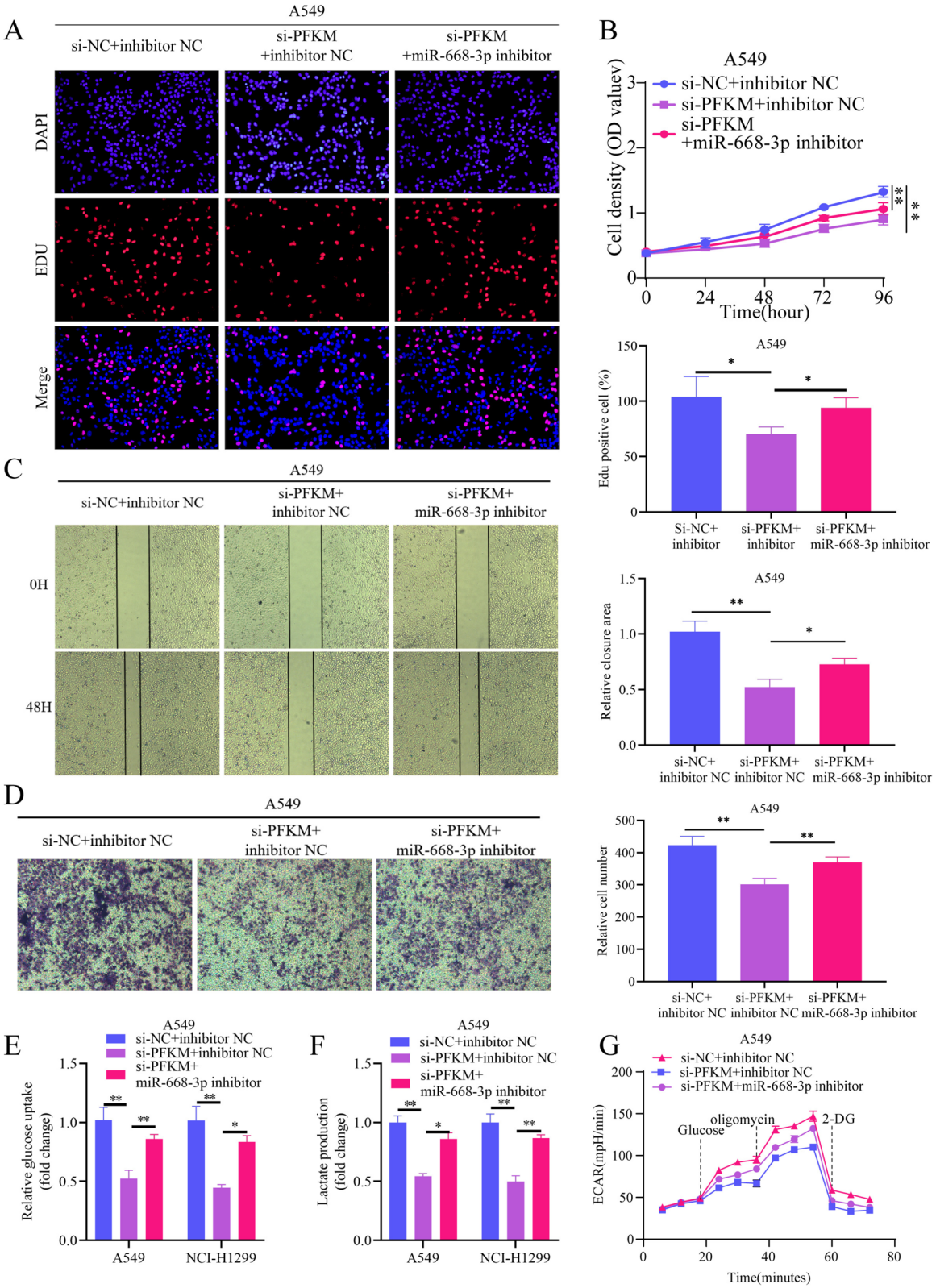

Fig. 7 PFKM reverses the anticancer effect of miR-668-3p in NSCLC. In A549 cells, transfection of si-NC + inhibitor NC, si-PFKM + inhibitor NC, and si-PFKM + miR-668-3p inhibitor was performed **A**, **B** Cell proliferation ability was detected by CCK-8 and EDU assays. **C**, **D** Wound healing and Transwell assays were conducted to measure cell migration and invasion in NSCLC cells. Scale bar, 100 μm. **E**, **F** Measurement of lactate and glucose uptake in NSCLC cells. **G** Analysis of extracellular acidification rate (ECAR) using a Seahorse analyzer. $^{*}P < 0.05$, $^{**}P < 0.01$, $^{***}P < 0.001$

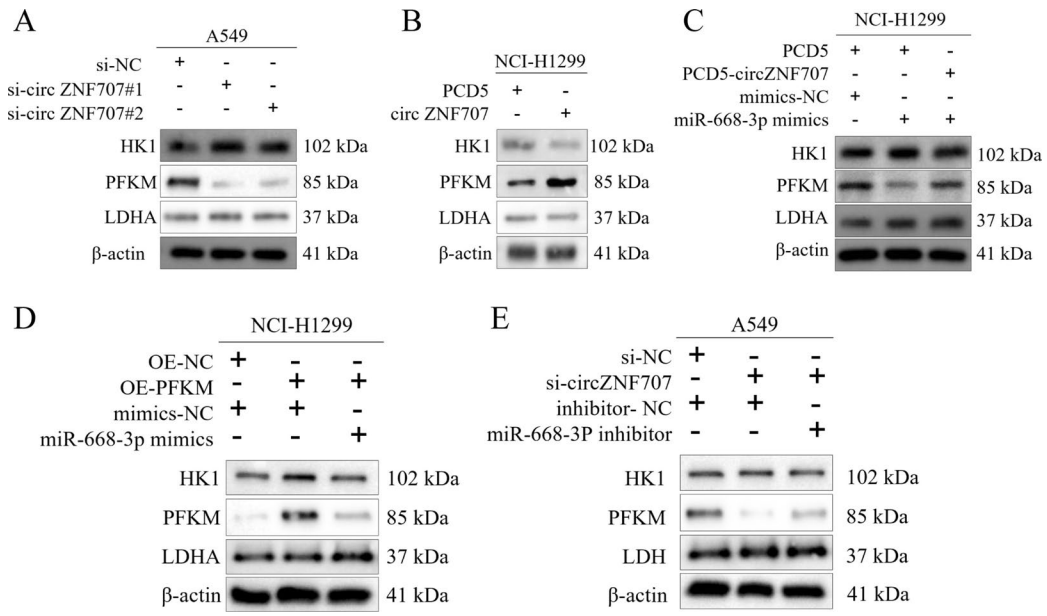

Fig. 8 circZNF707/miR-668-3p/PFKM axis promotes glycolysis in NSCLC cells. Western blot assay of PFKM, HK1, and LDHA proteins in NSCLC cells transfected with si-circZNF707 (**A**), PCD5-circZNF707 (**B**), PCD5-circZNF707 + miR-668-3p mimics (**C**), OE-PFKM + miR-668-3p mimics (**D**), and si-circZNF707 + miR-668-3p inhibitor (**E**)

subcellular localization study and discovered that circZNF707 is mostly located in the cytoplasm of NSCLC cells, indicating that it may be involved in controlling miRNA expression. We discovered a binding site between circZNF707 and miR-668-3p by using database software (miRanda, Circinteractome, and RNAhybrid) to identify probable miRNA binding sites of circZNF707. We identified a negative connection in their expression in NSCLC tissues and experimentally verified the targeting interaction between miR-668-3p and circZNF707. The inhibitory effects of miR-668-3p overexpression on cell proliferation, migration, and invasion may be reversed by overexpression of circZNF707.This work demonstrates miR-668-3p's capacity to inhibit the oncogenic effects of circZNF707 and offers the first evidence of the tumor-suppressive activity of miR-668-3p in NSCLC. Therefore, we suggest that circZNF707 interacts with miR-668-3p to perform its oncogenic effect. Through RNA sequencing and website prediction, we discovered that PFKM is a likely target of miR-668-3p, which we further verified in our tests. MiRNAs work by preventing the translation and destruction of target genes.

One of the rate-limiting enzymes regulating glycolytic flow is phosphofructokinase (PFK), a vital enzyme in the glycolytic energy metabolism pathway [26]. Changes in cellular metabolism are intimately correlated with its activity. Numerous studies have demonstrated that as compared to normal tissues or cells, the expression levels of PFK are much higher in tumour cells and tumour tissues [27, 28]. The rate of aerobic glycolysis in tumour cells likewise increases when PFK activity overall rises, meeting the increased synthetic metabolic demands of active tumour cells. Numerous oncogenes, including Myc, Ras, and HIF-1A, can also stimulate PFK activity [29]. According to our research, NSCLC tissues and cells co-express circZNF707 and PFKM, which compete with one another to bind miR-668-3p and control one another's expression. Functional studies show that PFKM has an oncogenic function, and that the target gene PFKM can inhibit miR-668-3p's ability to reduce tumour growth in NSCLC. Furthermore, circZNF707's oncogenic impact can be countered by downregulating PFKM. These

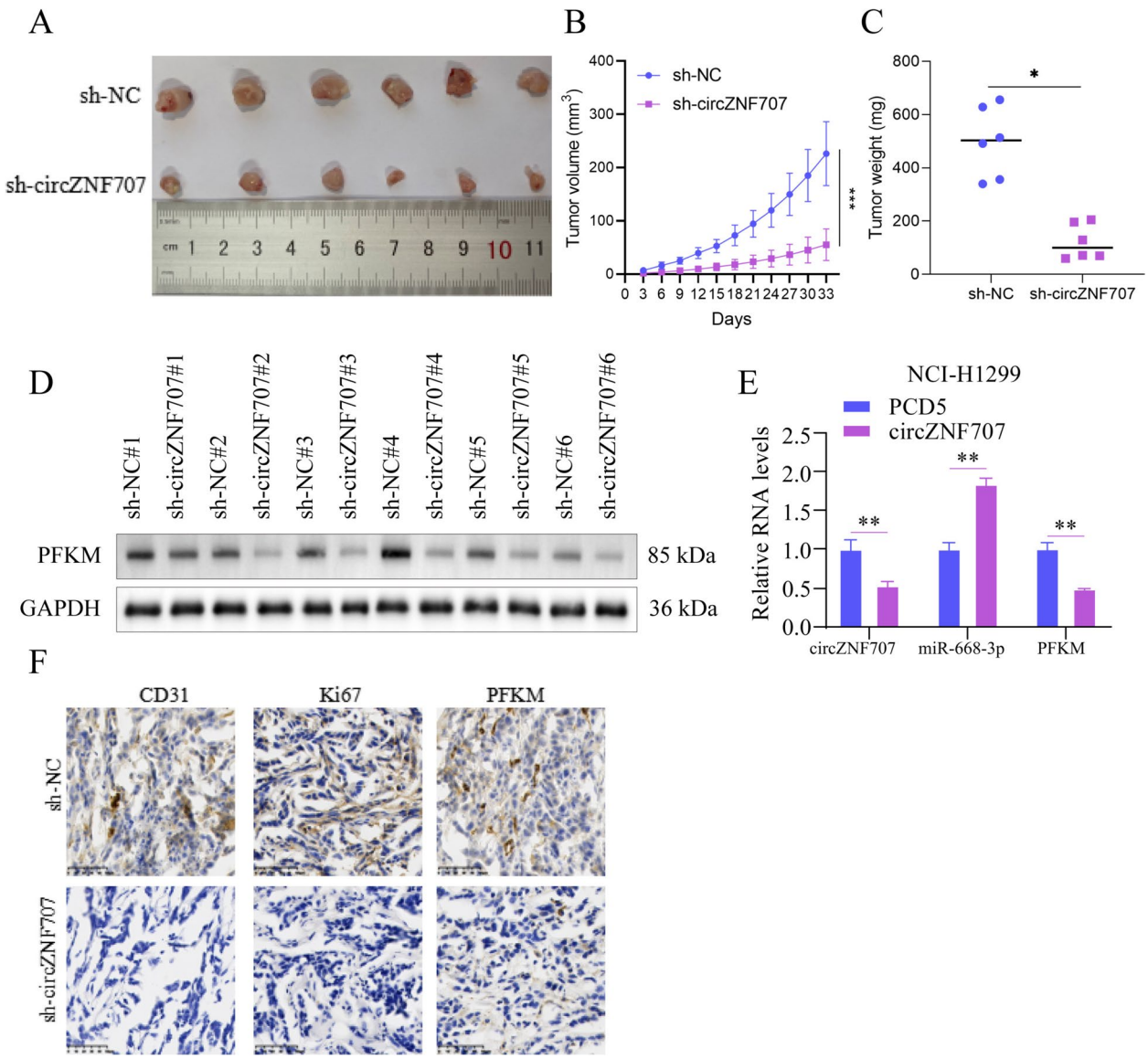

Fig. 9 Knockdown of circZNF707 inhibits the progression of NSCLC in vivo. **A** Representative images of subcutaneous tumor tissues in the sh-circZNF707 group and sh-NC group. **B**, **C** Tumor volume and weight of subcutaneous tumor tissues. **D** Western blot analysis of PFKM expression levels in subcutaneous tumor tissues of each group. **E** qRT-PCR analysis of circZNF707, miR-668-3p, and PFKM expression levels in subcutaneous tumor tissues of each group. **F** Immunohistochemical staining of PFKM, CD31, and Ki67 expression levels in subcutaneous tumor tissues of each group. Scale bar, 50 μm. *$P < 0.05$, **$P < 0.01$, ***$P < 0.001$

findings imply that the circZNF707/miR-668-3p/PFKM axis mediates the pro-tumorigenic effect of circZNF707 in NSCLC.

In summary, our research shows that the circZNF707-miR-668-3p-PFKM axis, which controls the proliferation, migration, invasion, and glycolysis of NSCLC cells, is part of a unique circRNA-miRNA-mRNA regulatory network in NSCLC cells. Our findings provide new insights into the diagnosis and treatment of NSCLC.

Supplementary Information

The online version contains supplementary material available at https://doi.org/10.1186/s40001-025-02359-z.

Supplementary material 1.

Supplementary material 2.

Supplementary material 3: Figure S1. The anticancer effect of si-circZNF707 in NSCLC can be reversed by miR-668-3p inhibitor. In A549 cells transfected with si-NC+miR-NC, si-NC+miR-668-3p inhibitor, and si-circZNF707+miR-668-3p inhibitor,CCK-8 and EDU experiments were performed to assess cell proliferation capability.Wound healing and Transwell assays were conducted to assess the migration and invasion ability of NSCLC cells. Scale bar, 100 μm. $^{*}P < 0.05$, $^{**}P < 0.01$.

Supplementary material 4: Figure S2. The anticancer effect of OE-PFKM in NSCLC can be reversed by miR-668-3p inhibitor. In NCI-H1299 cells, transfection of OE-NC+miR NC, OE-PFKM+miR NC, and OE-PFKM+miR-668-3p mimics was performedCell proliferation ability was detected by CCK-8 and EDU assays.Wound healing and Transwell assays were conducted to measure cell migration and invasion in NSCLC cells. Scale bar, 100 μm.Measurement of lactate and glucose uptake in NSCLC cells.Analysis of extracellular acidification rateusing a Seahorse analyzer. $^{*}P < 0.05$, $^{**}P < 0.01$, $^{***}P < 0.001$.

Supplementary material 5: Table S1 Primer sequences. Table S2 RNA oligonucleotide sequences. Table S3 Tissue samples and corresponding clinical parameters for this study.

Acknowledgements
Not applicable.

Author contributions
WC, SF, XZ and CZ designed the study. WC, SF, XW, TF and ZC performed experiments and analyzed data. WC, SF, YZ and WS wrote the main manuscript text. All authors read and approved the final manuscript.

Funding
This work was supported by Funds of the Ningbo Medical Science and Technology Plan Project (Grant Number No.2021Y14); Zhejiang Provincial Medical and Health Technology Plan (Grant Number No.2023RC084, No. 2022KY335, No.2023KY1112); the Ningbo Natural Science Foundation (Grant Number No. 2021J245) and Wu Jieping Medical Foundation.

Availability of data and materials
The datasets used and/or analysed during the current study are available from the corresponding author on reasonable request.

Declarations

Ethics approval and consent to participate
The First Affiliated Hospital of Ningbo University's Clinical Research Ethics Committee gave the study protocol approval (Approval No.: KS202112011). All experimental methods were carried out in compliance with the applicable laws. All animal experiments and procedures were approved and performed in accordance with the Animal Experimentation Ethics Committee of Ningbo University School of Medicine. This study was approved and performed by the Ethics Committee of the First Affiliated Hospital of Ningbo University.

Consent for publication
Not applicable.

Competing interests
The authors declare no competing interests.

Received: 17 December 2024 Accepted: 5 February 2025
Published online: 27 February 2025

References

1. Harada G, Yang SR, Cocco E, Drilon A. Rare molecular subtypes of lung cancer. Nat Rev Clin Oncol. 2023;20(4):229–49.
2. Passaro A, Jänne PA, Peters S. Antibody-drug conjugates in lung cancer: recent advances and implementing strategies. J Clin Oncol. 2023;41(21):3747–61.
3. Lahiri A, Maji A, Potdar PD, Singh N, Parikh P, Bisht B, Mukherjee A, et al. Lung cancer immunotherapy: progress, pitfalls, and promises. Mol Cancer. 2023;22(1):40.
4. Goodall GJ, Wickramasinghe VO. RNA in cancer. Nat Rev Cancer. 2021;21(1):22–36.
5. Chen LL. The expanding regulatory mechanisms and cellular functions of circular RNAs. Nat Rev Mol Cell Biol. 2020;21(8):475–90.
6. Zhou WY, Cai ZR, Liu J, Wang DS, Ju HQ, Xu RH. Circular RNA: metabolism, functions and interactions with proteins. Mol Cancer. 2020;19(1):172.
7. Arnaiz E, Sole C, Manterola L, Iparraguirre L, Otaegui D, Lawrie CH. CircRNAs and cancer: biomarkers and master regulators. Semin Cancer Biol. 2019;58:90–9.
8. Kristensen LS, Andersen MS, Stagsted LVW, Ebbesen KK, Hansen TB, Kjems J. The biogenesis, biology and characterization of circular RNAs. Nat Rev Genet. 2019;20(11):675–91.
9. Kristensen LS, Jakobsen T, Hager H, Kjems J. The emerging roles of circRNAs in cancer and oncology. Nat Rev Clin Oncol. 2022;19(3):188–206.
10. Liu Y, Liu Y, He Y, Zhang N, Zhang S, Li Y, Wang X, et al. Hypoxia-induced FUS-circTBC1D14 stress granules promote autophagy in TNBC. Adv Sci (Weinh). 2023;10(10):e2204988.
11. Li B, Zhu L, Lu C, Wang C, Wang H, Jin H, Ma X, et al. circNDUFB2 inhibits non-small cell lung cancer progression via destabilizing IGF2BPs and activating anti-tumor immunity. Nat Commun. 2021;12(1):295.
12. Shi X, Yang J, Liu M, Zhang Y, Zhou Z, Luo W, Fung KM, et al. Circular RNA ANAPC7 inhibits tumor growth and muscle wasting via PHLPP2-AKT-TGF-β signaling axis in pancreatic cancer. Gastroenterology. 2022;162(7):2004-17.e2.
13. Cheng Z, Yu C, Cui S, Wang H, Jin H, Wang C, Li B, et al. circTP63 functions as a ceRNA to promote lung squamous cell carcinoma progression by upregulating FOXM1. Nat Commun. 2019;10(1):3200.
14. Zhang N, Nan A, Chen L, Li X, Jia Y, Qiu M, Dai X, et al. Circular RNA circSATB2 promotes progression of non-small cell lung cancer cells. Mol Cancer. 2020;19(1):101.
15. Lv W, Tan Y, Xiong M, Zhao C, Wang Y, Wu M, Wu Y, et al. Analysis and validation of m6A regulatory network: a novel circBACH2/has-miR-944/HNRNPC axis in breast cancer progression. J Transl Med. 2021;19(1):527.
16. Liu Z, Zhou Y, Liang G, Ling Y, Tan W, Tan L, Andrews R, et al. Circular RNA hsa_circ_001783 regulates breast cancer progression via sponging miR-200c-3p. Cell Death Dis. 2019;10(2):55.
17. Xi Y, Shen Y, Wu D, Zhang J, Lin C, Wang L, Yu C, et al. CircBCAR3 accelerates esophageal cancer tumorigenesis and metastasis via sponging miR-27a-3p. Mol Cancer. 2022;21(1):145.
18. Xu S, Cheuk YC, Jia Y, Chen T, Chen J, Luo Y, Cao Y, et al. Bone marrow mesenchymal stem cell-derived exosomal miR-21a-5p alleviates renal fibrosis by attenuating glycolysis by targeting PFKM. Cell Death Dis. 2022;13(10):876.
19. Hackett EE, Charles-Messance H, O'Leary SM, Gleeson LE, Muñoz-Wolf N, Case S, Wedderburn A, et al. Mycobacterium tuberculosis limits host glycolysis and IL-1β by restriction of PFK-M via MicroRNA-21. Cell Rep. 2020;30(1):124–36.
20. van Zonneveld AJ, Kölling M, Bijkerk R, Lorenzen JM. Circular RNAs in kidney disease and cancer. Nat Rev Nephrol. 2021;17(12):814–26.
21. Li C, Ni YQ, Xu H, Xiang QY, Zhao Y, Zhan JK, He JY, et al. Roles and mechanisms of exosomal non-coding RNAs in human health and diseases. Signal Transduct Target Ther. 2021;6(1):383.
22. Yu T, Wang Y, Fan Y, Fang N, Wang T, Xu T, Shu Y. CircRNAs in cancer metabolism: a review. J Hematol Oncol. 2019;12(1):90.
23. Xiao MS, Ai Y, Wilusz JE. Biogenesis and functions of circular RNAs come into focus. Trends Cell Biol. 2020;30(3):226–40.
24. Li J, Sun D, Pu W, Wang J, Peng Y. Circular RNAs in cancer: biogenesis, function, and clinical significance. Trends Cancer. 2020;6(4):319–36.
25. Jie M, Wu Y, Gao M, Li X, Liu C, Ouyang Q, Tang Q, et al. CircMRPS35 suppresses gastric cancer progression via recruiting KAT7 to govern histone modification. Mol Cancer. 2020;19(1):56.

26. Jeon SM, Lim JS, Kim HR, Lee JH. PFK activation is essential for the odontogenic differentiation of human dental pulp stem cells. Biochem Biophys Res Commun. 2021;544:52–9.
27. Jourdain AA, Begg BE, Mick E, Shah H, Calvo SE, Skinner OS, Sharma R, et al. Loss of LUC7L2 and U1 snRNP subunits shifts energy metabolism from glycolysis to OXPHOS. Mol Cell. 2021;81(9):1905–19.
28. Zhou Y, Lin F, Wan T, Chen A, Wang H, Jiang B, Zhao W, et al. ZEB1 enhances Warburg effect to facilitate tumorigenesis and metastasis of HCC by transcriptionally activating PFKM. Theranostics. 2021;11(12):5926–38.
29. Gao W, Huang M, Chen X, Chen J, Zou Z, Li L, Ji K, et al. The role of S-nitrosylation of PFKM in regulation of glycolysis in ovarian cancer cells. Cell Death Dis. 2021;12(4):408.

Publisher's Note